Contents lists available at ScienceDirect

Journal of Molecular Structure

journal homepage: http://ees.elsevier.com

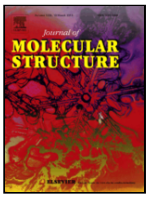

Bicyclo[1.1.1]Pentane as Phenyl Substituent in Atorvastatin Drug to improve Physicochemical Properties: Drug-likeness, DFT, Pharmacokinetics, Docking, and Molecular Dynamic Simulation

Radwan Alnajjar [a,b,*], Najwa Mohamed [c], Nagwa Kawafi [c]

[a] Department of Chemistry, Faculty of Science, University of Benghazi, Benghazi, Libya.
[b] Department of Chemistry, University of Cape Town, Rondebosch 7701, South Africa.
[c] Department of Medicinal Chemistry, Faculty of Pharmacy University of Benghazi, Benghazi, Libya

ARTICLE INFO

Article history:
Received 14 September 2020
Received in revised form 26 October 2020
Accepted 9 November 2020
Available online xxx

Keywords
Benzene bioisostere
MD
DFT
Bioavailability
Physicochemical properties

ABSTRACT

Hyperlipidemia influences on numerous diseases, such as atherosclerosis, hypertension, and diabetes mellitus, however it still treatable. Atorvastatin is one of the most common statins; yet, it has poor solubility due to the three phenyl rings, which lead to low bioavailability issues. Herein, we used bicyclo [1.1.1] pentane a benzene bioisostere as a replacement for these phenyl groups. In total, seven analogous **1_a**, **1_b**, **1_c**, **2_a**, **2_b**, **2_c**, and **3** were designed and investigated theoretically. Their drug-likeness, physicochemical properties, bioactivity, and pharmacokinetics properties were reported and analyzed. Further DFT calculations at CAM-B3LYP/6-31 + g in water were used to report the electronic properties and thermodynamic properties of the suggested analogues. Docking studied were conducted to mimic the interactions of the new derivatives with the active site of HMG-CoA reductase. Since docking results are not reliable, molecular dynamic simulations were carried out on analogous with the best docking score. Finally, binding free energy using MM-GBSA was calculated from the MD trajectories, reveals that compound **1_a** has promising properties as a drug with a docking score of -8.99 kcal/mol and MM-GBSA of -45.35 kcal/mol.

1. Introduction

Statins are a class of drugs that treat hyperlipidemia and known as HMG-CoA reductase inhibitors; this includes **atorvastatin**, fluvastatin, lovastatin, pitavastatin, pravastatin, rosuvastatin, and simvastatin.[1-3]

Atorvastatin (ATV) is a synthetic statin used for the treatment of low-density lipoprotein (LDL) cholesterol via the inhibition of HMG-CoA reductase, which is the main enzyme in the rate-limiting step in cholesterol synthesis via mevalonate pathway, Fig. 1. ATV has $IC_{50}$of 73, 102, and 106 nM toward HepG2 cells, human fibroblasts, and rat hepatocytes, respectively.[3-4]

Atorvastatin (7-(2-(4-fluorophenyl)-5-isopropyl-3-phenyl-4-phenylcarbamoyl)-1H-pyrrol-1-yl)-3,5-dihydroxy heptanoic acid), Fig. 2, was first identified and patented in 1985 by Bruce Roth. It was approved by the Food and Drug Administration (FAD) in 1996, for twelve years, from 1996 to 2012, the selling rate increased gradually under the name Lipitor. Atorvastatin became the drug number one for treating hyperlipidemia at that period, with more than 125 billion in sales in about 15 years. **Atorvastatin** has the highest-selling prescription drug around the Middle East, where it sold under trade names Torvast, Sortis, and Ator.[5]

Since ATV cans exist in liner or the acid form and closed or lactone form, Istvan et al. [6] resolve the crystal structure of the human HMGR bound to ATV at 2.22 Å, under crystallography examination, it indicates that the linear forms of **atorvastatin** are suitable for binding to the enzyme, as the terminal carboxylate group forms salt bridges with Lys692 and Lys735. In contrast, the hydroxy group serves as a charge-assisted hydrogen bond donor to Glu559 and as a hydrogen bond acceptor from Lys691 (Fig. 2). However, the structure of the active site of human HMG-CoA reductase in complex with products and with substrates has lately been clarified,[7] it produces little information concerning statin binding. The binding site of tetrameric HMG-CoA is symmetrical and made up of its chains A and B together, and chains C and D together. It was exposed through structural analysis of HMG-CoA that it has only one polypeptide chain with membrane-anchor, catalytic domains and linker. HMG-CoA reductase catalyzed the converting of HMG-CoA into mevalonate, creating mevaldehydeand mevaldyl-CoA as intermediates, using two NADPH + $2H^+$ molecules and releasing NADP + and CoA-SH during reduction.[8] The active site of the protein lays on its dimer edge, the dimer monomers are linked to a different substrates, one monomer is linked to HMG-CoA, and the other is

* Corresponding author.
E-mail addresses: Radwan.Alnajjar@uob.edu.ly (R. Alnajjar); Najwa.alshwihady86@gmail.com (N. Mohamed); Kawafinagwasaleh@gmail.com (N. Kawafi)

https://doi.org/10.1016/j.molstruc.2020.129628
0022-2860/

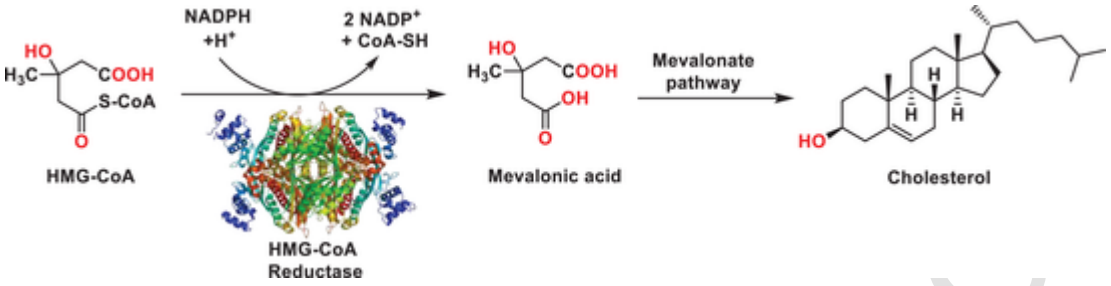

Fig. 1. Cholesterol synthesis pathway.

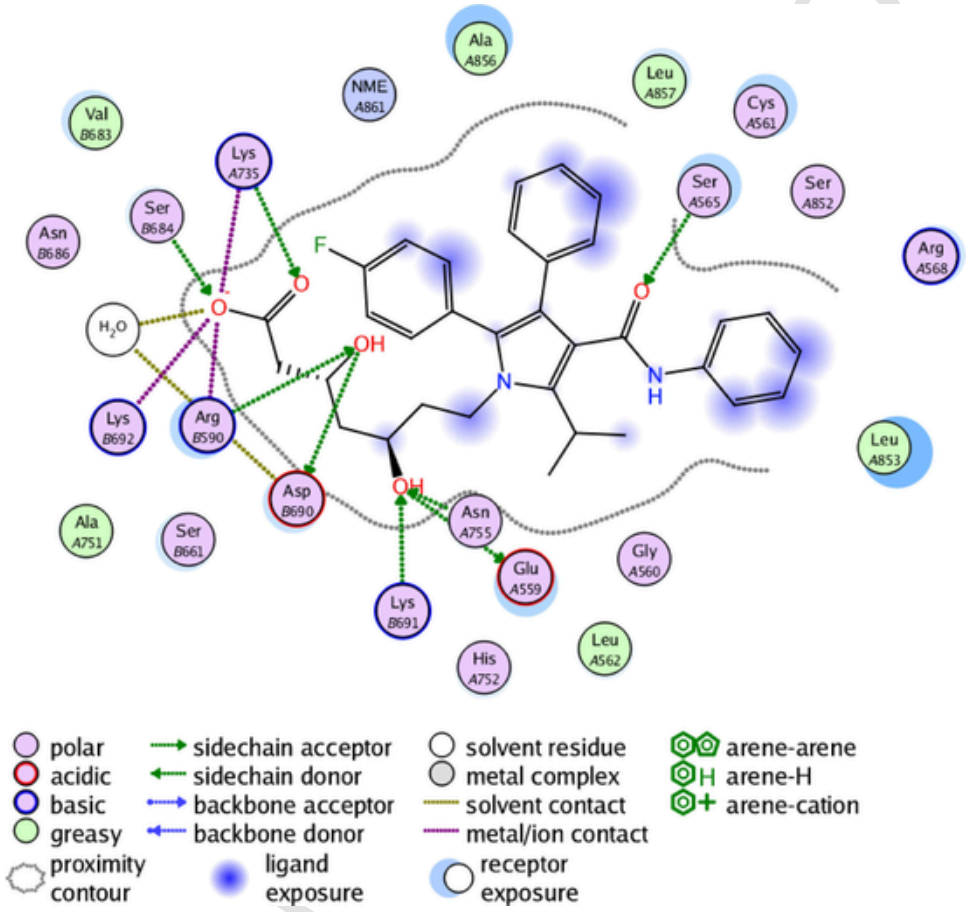

Fig. 2. Atorvastatin interactions within the active site obtained from the crystal structure.

linked to nicotinamide dinucleotide. It has a binding site with 3-dimensional wrinkle structurally comprising a nucleotide-binding design that is used for NADPH catalysis.[9] The four main catalytic amino acids, conserved in all HMGCR classes are glutamate, histidine, lysine, and aspartate.[10] The protonation of departure CoA thioanion is passed out via histidine (His866). CoA removal is essential as it could attack mevaldehyde and inhibit the completion of this finished process if it was reserved.[8] Lysine (Lys735, and Lys691), are including in formation the H-bonds with the carbonyl group of HMG-CoA and also contributes to steadying the mevaldyl-CoA intermediate.[11] Aspartates (Asp690, and Asp767) are also found within the active site, causal in two reductive processes of reaction, play a part in proton shuttle and hydrogen bonding. Whereas, in the second reductive process, mostly glutamate (Glu559) participates.[10] Other amino acids, for example, serine (Ser864), asparagine (Asn755), and tyrosine (Tyr479) as well as contribute in the catalytic action. These amino acids attach carboxylate group of HMG-CoA via forming hydrogen bonds, make hydrophobic pocket ended HMG-CoA and regulate HMGCR catalytic action.[12] It was established via docking studies that **atorvastatin** and its analogues form a complex with HMGCR via interacting with amino acids Arg590, Asn755, Glu559, Lys735, Lys691, Lys692 and Ser684 present in the active site of the same enzyme (Fig. 2) which is essential for catalysis, thus reducing the activity of the enzyme.[10] Although only the acid form lowers cholesterol levels, it has shown that drug interactions should be considered for both acid and lactone forms.

ATV shows a maximum plasma concentration after 60 – 120 minutes of oral administration, the bioavailability of **atorvastatin** (parent drug) is very low, approximately 14% and the systemic availability of HMG-CoA reductase inhibitory activity is around 30%, the low systemic bioavailability is probably due to the first-pass metabolism in the liver. **Atorvastatin** metabolized in *vivo* to ortho- and para- hydroxylated derivatives and several beta-oxidation products, while in *vitro* metabolism occurs by ortho- and para- hydroxylated metabolites which are equivalent to that of **atorvastatin**. Around 70% of the inhibition of HMG-CoA reductase attributed to active metabolites. CYP3A4 is also involved in the metabolism of **atorvastatin**.[13-14]

The molecular structure of **atorvastatin** is quite impressive, Briggs et al. [15] studied the crystallography of **atorvastatin** calcium salt [(**atorvastatin** ion)$_2$Ca], An et al. [16] found that there are three crystal forms of **atorvastatin** using powder X-ray diffractometry (PXRD), differential scanning calorimetry (DSC), and thermogravimetric analysis (TG), and Wang et al. [17] reported the NMR spectra of **atorvastatin** in the solid-state. Finally, Hoffmann[18] study the interconversion of hydroxy acid-lactone of **atorvastatin** using DFT methods. A molecular dynamics simulation, molecular docking, and 3D-QSAR studies by Wang[19] in 2014 included 120 fluorinated derivatives of **atorvastatin** shows that fluorinated derivatives have high HMGR inhibitory activity.[19]

In recent years, benzene bioisosteres groups such as bicyclo[1.1.1]pentane, bicyclo[2.2.2]octane, and cubane, have been introduced and used to improve potency, selectivity, physicochemical properties, bioavailability, and metabolic stability of bioactive compounds (Fig. 3). These groups able to reduce the aromatic property of the molecule, which is usually accompanied by lipophilicity, metabolic stability, and solubility problems, which lead to low bioavailability.[20-22]

Herein, we reported the bicyclo[1,1,1]pentane as a substituent for the phenyl group of **atorvastatin** in an attempt to overcome its poor solubility and bioavailability. Seven analogues were considered by replacing one phenyl group each time, then replacing two phenyl groups at the same time, finally replacing the three phenyl groups together, as shown in Fig. 4, their physicochemical properties and drug-likeness were evaluated and analyzed. Further, their electronic properties were studied at CAM-B3LYP/6-31 + g* level of theory in water to investigate the reactivity, thermodynamic stability and molecular electrostatic potential map behavior. Furthermore, these analogues were docked into the active site of the HMG-CoA reductase enzyme to get a hint on the interactions that they could make at the molecular level using the already available crystal structure of HMG-CoA reductase. Finally, molecular dynamic (MD) simulations were carried out on the best-docked drug-protein complexes to get a deep understanding of the affinity between the ligands and the HMG-CoA reductase active site in explicit solvent model for 100 ns to estimate their stability within the active site of the protein. These drug-protein complexes were then subject to the Molecular Mechanics /Generalized Born and Surface Area (MM/GBSA) calculations to estimate the corresponding relative binding free energies.

2. Materials and Methods

The drug ability was determined by the Lipinski, Ghose and Veber rules using Swiss ADME. Lipinski`s rules, also known as the "rule of 5" (RO5) supply a practical guide for detecting if a screened compound will be orally bioavailable. The Lipinski`s rules (RO5) states that molecules exhibition good absorption or permeation when they have an octanol-water partition coefficient (log P) < 5, molecular weight (MW) < 500, number hydrogen bond donors (n OH, NH) ≤ 5, number hydrogen bond acceptor (n O, N) ≤ 10.[23] The total number of violations

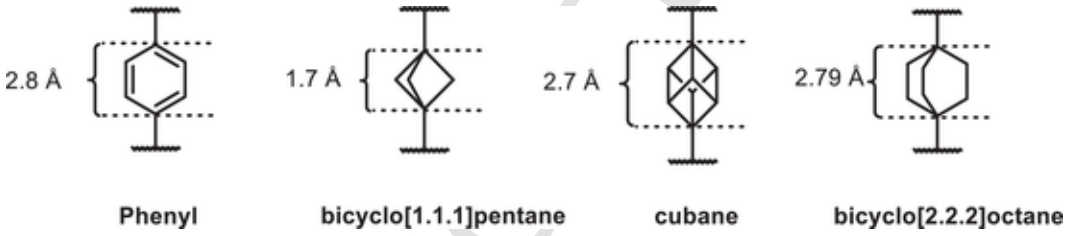

Fig. 3. Benzene bioisosteres.

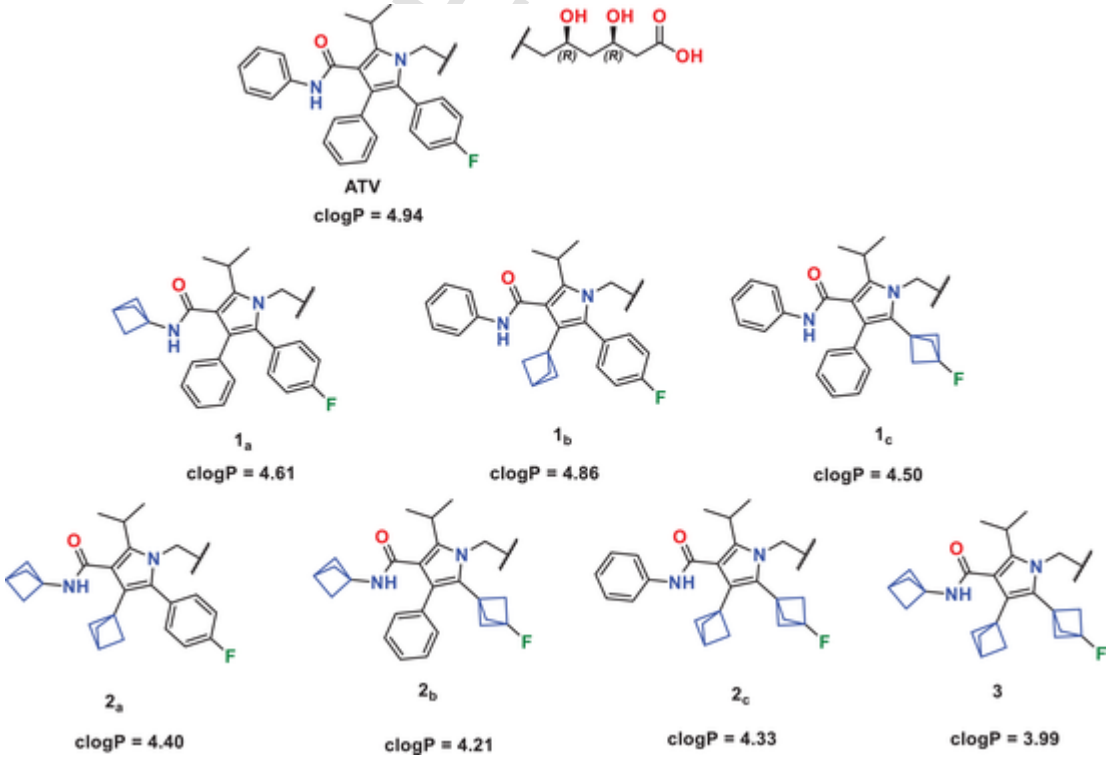

Fig. 4. The chemical structure of atorvastatin and its proposed bicyclo[1.1.1]pentane analogues.

Lipinski`s rules score, lies between '0' and '4'. Ghose et al. extended the work and established qualifying ranges for a logP (-0.4 to 5.6), molecular weight (160 to 480), and the number of atoms (20 to 70).[24] A study conducted by Veber on rats showed, molecular flexibility, topological polar surface area (TPSA), and hydrogen bonds count are important determinants for oral bioavailability. Veber`s rules for good bioavailability in rats, stating that the rotatable bonds ≤ 10, topological polar surface area (TPSA) ≤ 140 $Å^2$, and total H-bond donors and acceptors ≤ 12.[25]

Another important phenomenon that considers bioavailability is drug-likeness which evaluates qualitatively the chance for a compound to develop an oral drug with respect to bioavailability. Drug-likeness was recognized from chemical structural or physicochemical properties of progress compounds traditional enough to be measured oral drug-candidates. This idea is regularly employed to achieve filtering of small molecule libraries to eliminate molecules with properties most possibly incompatible with a suitable pharmacokinetic profile.[23] These SwissADME sections provide access to various rule-based filters, with different ranges of properties of which the molecule is distinct as drug-like. These filters frequently created from the investigation of leading pharmaceutical companies targeting to progress the quality of their proprietary chemical groups. The Lipinski filter 'rule-of-five', the Ghose (Amgen), Veber (GSK) methods were implemented from references [24-27], respectively. Molecules that violate more than one of these rules might have difficulties with bioavailability; consequently, these rules create some structural restrictions significant to the theoretical estimation of the oral bioavailability and is extensively used in discovering new drugs. However, this rule does not apply to natural substrates for such as cardiac glycosides, antibiotics, vitamins, and antifungals. The calculation outcomes presented in Table 2, shows that all the examined molecules obey Lipinski rules with ROF-Score ≤ 1 except the molecular weight, proposing that these molecules hypothetically could be suitable for oral administration. Compounds with ROF-Scores more than one are reflected to be marginal for additional improvement. Generally, when the bioactivity score is high, this will increase the probability of the considered compound to be active. Thus, a molecule having bioactivity score higher than 0.00 is most likely to possess numerous biological activities.

Pharmacokinetic properties which are carefully correlated with chemical structure, and practical information, can be saved and retrieved from computers database, these properties can be used to achieve computer-assisted in silico selections.[28] The predictions for passive human gastrointestinal absorption (GI Absorption) for the studied compounds reported in Table 3, shows that the analogue $\mathbf{2_b}$ and analogue **3** have a higher GI absorption than **atorvastatin**, analogues $\mathbf{1_{a\text{-}c}}$, and analogues $\mathbf{2_a}$,$\mathbf{2_c}$.

Additionally, the blood-brain barrier (BBB) provides homeostasis to the brain by protecting the brain from potentially harmful exogenous and endogenous materials. The ATP-binding cassette transporters (ABC-transporters) gene family are blood-brain barrier for various drug efflux transporters which increasingly known as significant determinants of drug distribution toward and removal from the CNS.

The ABC efflux transporters P-glycoprotein (Pgp) have been established as a central element of the BBB that can actively transport an enormous different of lipophilic drugs outside of the brain capillary endothelial cells that form the BBB.[29] Blood-brain permeation barrier (BBB permeant) showed that all compounds could not cross BBB. As it is known, this is important for decreasing the central nervous system (CNS) side effects. Furthermore, it is crucial to understand the interaction of small molecules with cytochromes P450 (CYP) isoenzymes which are the essential enzymes included in Phase I biotransformation. An indispensable role in biotransformation including CYP3A4, CYP2D6, CYP2C9, CYP2C19 and CYP1A2. Induction and inhibition of CYP isoenzymes induced by drugs are significant and clinically applicable pharmacokinetic mechanisms of drug interactions. Also, this superfamily of isoenzymes is the leading player in drug excretion via metabolic biotransformation.[30] Inhibition of these isoenzymes is indeed one leading cause of drug-drug interactions leading to adverse effects due to the decrease excretion and buildup of the drug or its metabolites,[31] many inhibitors of the CYP isoforms have been recognized, certain are affecting various CYP isoforms, whereas other inhibitors exhibited selectivity for specific isoenzymes.

Docking was used to studying the interaction of ligand-protein interactions; however, docking protocols are usually fast and approximated and lacks protein flexibility, which may affect the consistency of the resulting ligand-protein complex. Therefore, a more computationally expensive but more precise molecular dynamic simulations methods may provide a better complementary with docking. In general, MD simulation used to study the macromolecule behavior, and it is constructed on classical mechanics and using Newton's equation of motion to calculate the position of and speed of each atom of the studied structure. Taking into account the facts mentioned earlier; molecular dynamic simulations were carried out using Desmond package on the ligand-protein complexes to mimic the interaction of these drugs with human HMG-CoA reductase enzyme active site for 100 ns. Only compounds with high docking score were selected for MD simulations; this includes $\mathbf{1_a}$, $\mathbf{2_b}$, and **atorvastatin** as reference.

Finally, the average binding energy was calculated for equilibrated MD trajectory, 200 snapshots were selected with a 50 ps interval for further analysis. The binding energy was calculated according to the equations:

$$\Delta G_{bind} = \Delta E_{MM} + \Delta G_{solv} + \Delta G_{SA}$$

Where ΔE_{MM} is the difference in minimized energies between complex, ligand, and protein-energy as following:

$$\Delta E_{MM} = E_{(complex)} - E_{(ligand)} - E_{(receptor)}$$

ΔG_{solv} denotes the difference in GBSA solvation energy of the complex and the sum of ligand and protein solvation energies. At the same time, ΔG_{SA} is the differences in surface area energy of the complex and the sum of protein and ligand.

The average MM-GBSA binding energy was generated using the thermal_mmgbsa.py python script provided by Schrodinger which also generate Coulomb energy, Covalent binding energy, Van der Waals energy, Lipophilic energy, Generalized Born electrostatic solvation energy, Hydrogen-bonding energy. All the obtained data are reported in kcal/mol and shown in Table 7.

3. Computational and theoretical details

3.1. DFT Calculations

The initial structure of **atorvastatin** was extracted from the crystal structure of human HMG-CoA reductase enzyme, which was obtained from the protein data bank (PDB code: 1HWK)[6]. Further, the structure was modified, and the resultant structures were optimized at PM6 followed by CAM-B3LYP/6-31 + g* in water as a solvent, the solvent was implemented using the polarizable continuum model(PCM), all structures were confirmed to be minima with no imaginary frequency present. All thermodynamic parameters including, energy (ΔE), enthalpy (ΔH), Gibbs free energy (ΔG), and entropy (S) were reported. The electronic properties such as E_{HOMO}, E_{LUMO}, the energy gap between LUMO and HOMO, global hardness ($\eta = I\text{-}A/2$), electronegativity ($\chi = I + A/2$), electronic chemical potential ($\mu = -(I + A)/2$), and electrophilicity ($\omega = \mu^2/2\eta$) were also evaluated and analyzed.

3.2. Docking Study

A database of the suggested compounds along with **atorvastatin** was build using molecular operative environment MOE 2015 suite[32]. The database structures were minimized, protonated, and their charges fixed using Structure Preparation Panel implemented in MOE at Am-

ber10 forcefield. The crystal structure 1HWK was also prepared using the same panel at the Amber10 forcefield as well, this was followed by removing crystal water except for active site (4.5 Å were considered). Chains C and D were deleted from workspace along with their heteroatoms and water molecules. Chains A and B were only considered for docking. Triangle matcher was selected as placement methodology and London dG as the scoring methodology. The rigid receptor was used as a refinement methodology, and the scoring method was chosen to be GBVI/WSA dG to select the best ten poses from 100 different ones for each compound. The eight ligands MDB file was loaded, and general dock calculations were automatically run. The resulted poses were studied carefully after completion, and the best ones with the highest scores were selected. Moreover, in the beginning, a validation process was performed by docking only the co-crystallized inhibitor in the target protease, and a good performance was indicated by low RMSD (0.90) values between docked and crystal conformations.

3.3. Molecular Dynamic

The Molecular dynamic simulations were carried out using Desmond simulation package of Schrödinger LLC.[33] The NPT ensemble with a temperature of 300 K and a pressure 1 bar was applied in all runs. The simulation length was 100 ns with a relaxation time one ps for all selected ligands. The OPLS3 force field parameters were used in all simulations.[34] The cutoff radius in Coulomb interactions was 9.0 Å. The orthorhombic periodic box boundaries were set 10 Å away from the protein atoms., The water molecules were explicitly described using the transferable intermolecular potential with three points (TIP3P) model.[35-36] Salt concentration set to 0.15 M NaCl and was built using the System Builder utility of Desmond.[37] The Martyna–Tuckerman–Klein chain coupling scheme with a coupling constant of 2.0 ps was used for the pressure control and the Nosé–Hoover chain coupling scheme for the temperature control.[38-39] Nonbonded forces were calculated using a RESPA integrator where the short-range forces were updated every step and the long-range forces were updated every three steps. The trajectories were saved at 20 ps intervals for analysis. The behavior and interactions between the ligands and protein were analyzed using the Simulation Interaction Diagram tool implemented in Desmond MD package. The stability of MD simulations was monitored by looking on the RMSD of the ligand and protein atom positions in time.

3.4. MD Trajectory Analysis and Prime MM-GBSA Calculations

Simulation interactions diagram panel of Maestro software was used to monitoring interactions contribution in the ligand-protein stability. The molecular mechanics generalized born/solvent accessibility (MM – GBSA) was performed to calculate the ligand binding free energies and ligand strain energies for docked compounds over the 100 ns period with thermal_mmgbsa.py python script provided by Schrodinger which takes a Desmond trajectory file, splits it into individual snapshots, runs the MM-GBSA calculations on each frame, and outputs the average computed binding energy.

3.5. Physicochemical Properties

Physicochemical properties and bioactivity were calculated using SwissADME (www.swissadme.ch) and Molinspiration (www.molinspiration.com)

4. Result and Discussion

4.1. Evaluation of drug-likeness (drug ability)

Physicochemical properties including molecular weight (MW), molecular refractivity (MR), polar surface area (PSA), partition coefficient (log $P_{o/w}$) hydrogen bond acceptors and donors counts, volume, and the number of rotatable bonds in a molecule count of specific atom types are collected in Table 1.

Drug-likeness can be assumed as a right balance between molecular parameters that affecting pharmacokinetics and pharmacodynamics of molecules which finally affects their absorption, distribution, metabolism, and excretion (ADME) in the human body like a drug. Additionally, from the rule of five, the molecular mass of drugs should be <500. The molecular masses of all compounds (**atorvastatin, $\mathbf{1_{a\text{-}c}}$, $\mathbf{2_{a\text{-}c}}$,** and **3**) are more than 500 (558.64, 548.64, 538.65, and 528.66) respectively, that makes it challenging to cross membranes, transport, absorb and diffuse compared to small molecules.[40] Molecular refractivity (MR) is an important condition to detect the steric factor. It is typically selected as a straightforward measure of the volume employed either via a single atom or a group of atoms.[41] Molecular refractivity (MR) values were 158.26, 152.08,152.67, 152.80, 146.49, 146.62, 147.21 and 141.03 for **atorvastatin** and its analogues respectively, that means molecular refractivity rise with the increase of the molecular weight of the **atorvastatin** and its analogues. Another important parameter which was calculated using the fragmental technique called topological polar surface area (TPSA), considering oxygen and nitrogen as polar atoms, wis an essential useful parameter used for estimation properties of drug transportation. This parameter has been observed to associate very well with the human blood-brain barrier penetration, bioavailability, and intestinal absorption. Lipinski, Ghose and Veber rules say that topological polar surface area (TPSA) should be lower than 140 $Å^2$.[42] The considered bicyclo[1.1.1]pentane substituents did not affect the TPSA as it can see in Table 1 (111.79), this means that the new derivatives will have excretion time similar to **atorvastatin.** The partition coefficient between *n*-octanol and water (log $P_{o/w}$) is the traditional property for lipophilicity estimation. It has a whole section in SwissADME because of the crucial importance of this physicochemical character for pharmacokinetics drug discovery.[43] Several computational techniques for log Po/w determination were developed with varied performance on different chemical groups. General practice

Table 1
Physiochemical properties for atorvastatin and its Analogues.

Compound	MW	MR	TPSA	CIogP	IogS	nRotb	HBD	HBA	Volume
ATV	558.64	158.26	111.79	4.94	-7.77	13	4	6	513.80
$\mathbf{1_a}$	548.64	152.08	111.79	4.61	-6.22	13	4	6	504.45
$\mathbf{1_b}$	548.64	152.67	111.79	4.86	-6.90	13	4	6	504.45
$\mathbf{1_c}$	548.64	152.80	111.79	4.50	-6.19	13	4	6	504.12
$\mathbf{2_a}$	538.65	146.49	111.79	4.40	-6.08	13	4	6	495.09
$\mathbf{2_b}$	538.65	146.62	111.79	4.21	-5.36	13	4	6	494.77
$\mathbf{2_c}$	538.65	147.21	111.79	4.33	-6.06	13	4	6	494.77
3	528.66	141.03	111.79	3.99	-5.23	13	4	6	485.41

nRotb: number of rotatable bonds; HBD: number of hydrogen bond donor; HBA: number of hydrogen bond donor-acceptor.

Table 2
Drug likeness score for atorvastatin and its Analogues

	Lipinski	Ghose	Veber	Bioavailability score
ATV, 1_a, 1_b, and 1_c	Yes; 1 violation MW > 500	No;4 violation MW > 480 WLOGP > 5.6 MR > 130 # of atoms > 70	No; 1violation: Rotors > 10	0.56
2_a, 2_b, 2_c, and 3	Yes; 1 violation: MW > 500	No; 3 violations: MW > 480, MR > 130, #atoms > 70	No; 1 violation: Rotors > 10	0.56

Table 3
Pharmacokinetics for atorvastatin and its Analogues.

Compounds	GI Absorption	P-gp substrate	CYP2C19 inhibitor	CYP2D6 inhibitor	Log K_p
ATV	Low	Yes	Yes	Yes	-6.19
1_a	Low	Yes	Yes	Yes	-6.69
1_b	Low	Yes	Yes	Yes	-6.22
1_c	Low	Yes	Yes	No	-6.71
2_a	Low	Yes	Yes	No	-6.72
2_b	High	Yes	Yes	No	-7.21
2_c	Low	Yes	Yes	No	-6.74
3	High	No	No	No	-7.25

is usage numerous predictors to select the best accurate method for given chemical groups or to create consensus determination. The models after the predictors must be as different as possible to rise the predication accuracy through consensus log Po/w.[44] The lipophilicity is potentially linked to toxicity, which agrees with the observation that lipophilic binding is non-specific, whereas polar binding is related to the specificity and therefore selectivity. It is proof that the toxicity is significantly higher for compounds with log $P_{o/w} > 5$ and TPSA < 75 Å^2.[45]

The log$P_{o/w}$ value of the compounds are showed to be 4.94, 4.86, 4.50, 4.40, 4.21, 4.33, and 3.99 (Table 1) which follows Lipinski`s rule of five**.** Proposed compounds are likely to have adequate hydrophilicity as well as adequate lipophilicity, which shows that these compounds will have good permeability across cell membranes. The solubility of molecules can significantly simplify the drug development process, mainly the ease of formulation.[46] Furthermore, for drug discovery methods of oral administration, solubility is one main property affecting absorption.[47] As well as, a drug designed for parenteral treatment has to be greatly water-soluble to deliver an adequate amount of active ingredient in the smallest volume from the pharmaceutical dosage form.[48] However, the chemical structures of these molecules (Fig. 4) indicate that analogue **3** is the most hydrophilic compound, followed by analogues **$2_{a\text{-}c}$**, then comes analogues **$1_{a\text{-}c}$** and lastly, **atorvastatin**. As noted from Table 1, bicyclo[1.1.1]pentane can increase the solubility via eliminating the π – π interactions within the molecule and increasing the nonplanarity of the molecule which led to reduce the lattice energy of the drug crystal. The number of hydrogen bond donors and acceptors (HBD, HBA) for all molecules obey Lipinski's rule for drug-likeness, which is smaller than five for hydrogen donors and smaller than ten for hydrogen acceptors. Finally, results expose that all proposed analogues**$1_{a\text{-}c}$, $2_{a\text{-}c}$**, and **3** obeyed Lipinski with one exception, but did not follow its extension rules.

For bioavailability compounds with -0.50 to 0.00 values are expected to be moderately active, and if the score is less than -0.50, it is presumed to be inactive. All proposed derivatives have bioavailability higher than zero (0.56), which suggest that they are bioactive.

4.2. Pharmacokinetics

From the previous results, it notices that proposed **atorvastatin** analogues have physicochemical properties within the acceptable value. Thus, these parameters should be taken into consideration as indicators for more screening investigates against various targets including G-protein-coupled receptors (GPCR), Protease inhibitor (PI), Kinase inhibitor (KI), Ion channel modulator (ICM), Nuclear receptor ligand (NRL), and Enzyme inhibitor (EI); therefore, via using SwissADME, the bioactivity of all compounds were validate and reported in Table 3.

Consequently of excessive importance for drug discovery to estimate the affinity with which the molecule will cause significant drug-drug interactions through inhibition of CYPs, and to regulate which isoforms are inhibited.[49] SwissADME permits the estimation for a molecule to be a substrate of P-gp or inhibitor of the most significant CYP isoenzymes. Taken the obtained results into account, we observed the following: **atorvastatin** and its analogues cannot inhibit CYP1A2 and are not BBB permeant, **atorvastatin** and its analogues were able to inhibit CYP2C9 and CYP3A4. **Atorvastatin** and its analogues have permeability glycoprotein (P-gp)except analogue **3, atorvastatin** and analogues inhibited CYP2C19 whereas analogue **3** could not. **Atorvastatin** and analogues **$1_{a\text{-}b}$** were able to inhibit CYP2D6, while other analogues could not inhibit it. Another important model is a multiple linear regression that purposes at expecting the skin permeability coefficient (K_p). It is modified from Potts and Guy,[50] who establish K_p linearly associated with lipophilicity and molecular size. The high negative log K_p (with K_p in cm/s), the lower the skin permeant of the compound. From Table 3, the more negative value is Analogue **3** (-7.25) that is meaning it has low skin permeant, followed by analogue **$2_{a\text{-}c}$**, analogue **$1_{a\text{-}c}$**, and **atorvastatin**, respectively.

5. Density functional theory (DFT)

The optimized geometries of compounds **1_a, 1_b, 1_c, 2_a, 2_b, 2_c**, and **3** were obtained at CAM-B3LYP/6-31 + g* level of theory using Gaussian 09 software, the optimized geometries are presented in Fig. 5. Since our interest was about the structural properties of the analogues and the effect of the substituents on the electronic properties, these properties were obtained (Table 4) and analyzed.

5.1. Electronic properties

The electronic properties of the suggested compounds such as global hardness (η), the electronic chemical potential (μ), and electrophilicity index (ω)are listed in Table 4. The global hardness (η) parameter is related to the energy gap ($E_g = E_{LUMO} - E_{HOMO}$) and defined as the measurement from the resistance of an atom or a group of atoms to charge transfer. The E_g is an essential parameter for determination of the reactivity of the compounds. The electronic transport at the molecule with a low gap is more accessible. A molecule with a low E_g has a high chemical reactivity, low kinetic stability and is a soft molecule; whereas a hard molecule has a large E_g.[51] The E_g of the suggested derivatives was in the range of -7.19 eV and -6.99 eV which is quite similar to **atorvastatin,** and it indicates good stability of these compounds. The electrophilicity index (ω) shows that **atorvastatin** and its derivatives are poor electrophiles (ω < 1.50 eV).[52]

The total energy, relative enthalpy, relative Gibbs free energy, relative entropy, and dipole moment for suggested compounds are reported in Table 5. As it can be seen from Table 5, whenever one substation is taking place, it will be preferred to substitute the 4-fluoro phenyl which

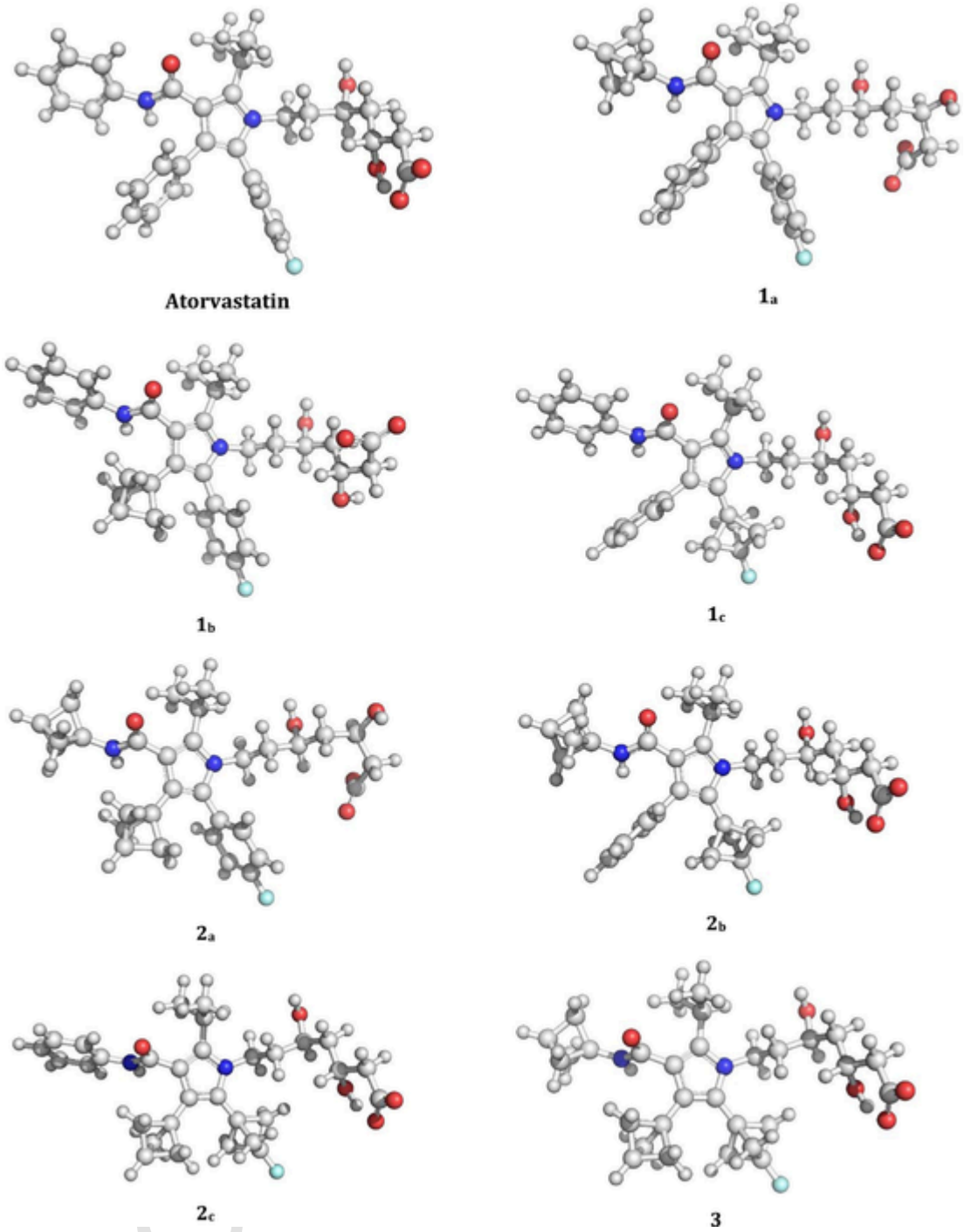

Fig. 5. Optimized structures of atorvastatin and its analogues at CAM-B3LYP/6-31 + G*/water.

leads to $\mathbf{1_c}$, this analogue shows stability by about 10.86 kcal/mol and 12.44 kcal/mol compared to $\mathbf{1_a}$and $\mathbf{1_b}$, respectively. Whenever a two substitution is taking place, 2b found to be the most stable analogue among others, and it was more stable then $\mathbf{2_a}$ by 14.07 kcal/mol and $\mathbf{2_c}$ by 7.34 kcal/mol. The position of the bicyclo[1.1.1]pentane also affect the polarity of the molecule; the dipole moment fluctuates between 30.95 and 36.68 D which still in acceptable range compared to **atorvastatin** which showed a dipole moment of 34.28 D.

5.2. Frontier molecular orbitals

Frontier molecular orbitals (FMO) provide insight into the active moiety of the molecule. Usually, the HOMO orbital is associated with the nucleophilic property while the LUMO is associated with the electrophilic property of the molecule. The frontier molecular orbitals of all studied compounds are presented in Fig. 6. Examination the FMO of the suggested analogues, reveals that HOMO orbitals did not come across any change with respect to **atorvastatin** HOMO which localized on the pyrrole ring of the molecule with a small contribution to the fluorophenyl moiety. The LUMO on the other side is affected by introduc-

Table 4
The calculated electronic properties of atorvastatin and its analogues at CAM-B3LYP/6-31 + G*/water

	E_{HOMO} (eV)	E_{LUMO} (eV)	E_g (eV)	η (eV)	μ (eV)	ω (eV)
ATV	-7.20	0.25	7.45	7.45	-3.47	0.81
$\mathbf{1_a}$	-7.15	0.37	7.52	7.52	-3.39	0.76
$\mathbf{1_b}$	-7.17	0.32	7.49	7.49	-3.43	0.78
$\mathbf{1_c}$	-7.19	0.28	7.47	7.47	-3.46	0.80
$\mathbf{2_a}$	-7.13	0.46	7.59	7.59	-3.33	0.73
$\mathbf{2_b}$	-7.17	0.57	7.74	7.74	-3.30	0.70
$\mathbf{2_c}$	-7.03	0.39	7.42	7.42	-3.32	0.74
3	-6.99	0.73	7.72	7.72	-3.13	0.63

Table 5
Relative energies, enthalpy, Gibbs, and entropy of atorvastatin and its analogues at CAM-B3LYP/6-31 + G*/water

	E°	ΔE	ΔH	ΔG	ΔS	μ
	(a.u)	(kcal/mol)	(kcal/mol)	(kcal/mol)	(cal/mol K)	(D)
ATV	-1862.81414	-	-	-	247.98	34.28
$\mathbf{1_a}$	-1825.83423	10.83	10.23	8.32	247.82	30.95
$\mathbf{1_b}$	-1825.83166	12.44	12.01	11.08	244.55	33.40
$\mathbf{1_c}$	-1825.85149	**0.00**	**0.00**	**0.00**	241.41	35.95
$\mathbf{2_a}$	-1788.86130	14.07	13.71	13.07	241.98	30.30
$\mathbf{2_b}$	-1788.88371	**0.00**	**0.00**	**0.00**	239.84	36.07
$\mathbf{2_c}$	-1788.87202	7.34	7.82	8.55	237.39	36.21
3	-1751.90407	-	-	-	233.58	36.68

ing the bicyclic moiety; the **atorvastatin** LUMO was localized on the phenyl ring with a small contribution to fluorophenyl and phenyl carbamoyl, $\mathbf{1_a}$, $\mathbf{1_c}$, and $\mathbf{2_b}$ LUMO were the same as **atorvastatin** since the phenyl group was present in these analogues. Removing the phenyl group led to a shift in LUMO localization, analogues $\mathbf{1_b}$ and $\mathbf{2_a}$ LUMO localized on the fluorophenyl group instead of the missing phenyl. On the other hand, removing both phenyl and fluorophenyl result in the localization of the of $\mathbf{2_c}$'s LUMO on the phenyl carbamoyl moiety of the molecule, Finally, removing phenyl, fluorophenyl, and the phenyl of phenyl carbamoyl moiety led to localization of the LUMO of analogue **3** on the carbonyl group and the nitrogen atom of the carbamoyl moiety. These change in LUMO may be directed to different metabolite in the metabolism of the suggested analogues.

5.3. Molecular Electrostatic Potential (MEP) analysis

Molecular electrostatic potential (MEP) maps were used to identify the negative and positive sites of electrostatic potentials for electrophilic and nucleophilic reactions. The color of the surface represents the difference in electrostatic potential. Blue is referring to the most positive region followed by green, while yellow, orange and red represent the negative regions with red being the most negative. The MEPs of the suggested compounds were computed at CAM-B3LYP/6-31 + G*/H_2O level of theory (Fig. 7). As can be seen from Fig. 7, the carboxyl group has the highest electron density, while the phenyl groups and the bicyclic moiety shows neutral characters, in general, it evident that the MEP map did not affect when the phenyl ring was substituted into bicyclic rings.

6. Docking studies

The technique of molecular docking is an important tool used in computer-aided drug discovery and structural biology in describing and determining the compatible interaction of ligands with the specific target protein.[53] In this study, to investigate the binding situation in which the ligand interacts within the HMG-CoA, molecular docking studies were performed on atorvastatin and its analogues. All docking scores were reported in Table 6.

All molecules were docked within the active site of 1HWK; the highest binding affinity score and the best pose was chosen for each molecule. The binding affinities of compound $\mathbf{1_a}$ and $\mathbf{2_b}$ against 1HWK are -8.99, and -8.70 kcal/mol, respectively. These binding affinities are slightly higher than that of **atorvastatin**. No bicyclic moiety bond is detected for modified analogues Fig. 8. Whereas the aliphatic side chain plays an important role in binding with the active site of the enzyme, thus it can form up to six hydrogen bonds with amino acid residues. For example, the dock of compound $\mathbf{1_a}$ with 1HWK crystal structure describes in Fig. 8, it is simply seen that two main amino acids (Glu559, and Lys735) of 1HWK interact with the compound $\mathbf{1_a}$ via hydrogen bonding, with a distance of 2.35 Å, and 2.50 Å, respectively. Notably, compound $\mathbf{1_a}$ was also able to form a hydrogen bond with Asp690 with 3.86Å using crystal water as a bridge. Compound $\mathbf{2_b}$ has a good score (-8.70kcal/mol), due to its ability to form six hydrogen bonds with (Glu559, Arg590, Lys735, Asn755, Lys691, and Lys735), compound $\mathbf{1_b}$come next with ability to form five hydrogen bonds with (Lys735, Ala751, Asn755, Lys691, and Lys692) resulting in -8.54 kcal/mol score.

Interestingly, the affinity binding score of compounds $\mathbf{1_c}$ and $\mathbf{2_c}$were -7.60 kcal/mol for both, so it is smaller than the compounds mentioned above, the two compounds could form a hydrogen bond with Lys735 and Asp690 via water bridge. Compound $\mathbf{1_c}$ forms another hydrogen bond with Lys692 through crystal water like a bridge, whereas compound $\mathbf{2_c}$ was able to create another hydrogen bond with Lys691.

Compounds $\mathbf{2_a}$ and **3** showed the lowest binding affinity with a docking score of-7.32, -7.54kcal/mol, respectively. Compound $\mathbf{2_a}$ was able to make only three hydrogen bonds with Asp690, Lys735, and Lys691, while compound **3** forms two hydrogen bonds with Lys735 and Asn755, as illustrated in Table 6 and Fig. 8.

In conclusion the docking score was in the following order: $\mathbf{1_a} > \mathbf{2_b} >$ ATV $> \mathbf{1_b} > \mathbf{1_c}, \mathbf{2_c} > \mathbf{3} > \mathbf{2_a}$.

7. Molecular Dynamics simulation

7.1. Protein and ligand RMSD analysis

To monitor the effect of the molecules on the conformational stability of HMG-COA reductase during simulations, RMSD values of Cα atoms were estimated for all the complexes with respect to the initial structure. The results were plotted as a function of the simulations time in Fig. 9a. As can be seen in the plots, all the complexes tend to reach their stable states after 40 ns, the fluctuation of the proteins were within acceptable variation with RMSD less than 3.00 Å indicating the stability of protein conformation.

The RMSD of ligands were also plotted as a function of simulation time to display the RMSD of a ligand that is aligned and measured just on its reference conformation within the active site. As it can be seen from Fig. 9b, analogue$\mathbf{1_a}$ was stable within the actives site and showed similar stability like the **atorvastatin** shows. On the other hand, analogue$\mathbf{2_b}$ was ultimately loose and moved almost 7 Å from its original position before reaching equilibrium at 30 ns; even though it was fluctuating within the new site by around 3 Å.

$\mathbf{2_b}$ did not leave the active site completely; still, instead, it just flips its orientation within the active site, the nature of ligand interaction with the active site depends entirely on the aliphatic side chain of the ligand which able to form multiple hydrogen bonds with active site residues. In case of **atorvastatin** and $\mathbf{1_a}$, it looks like the volume of the molecule did not change a lot, in contrast to $\mathbf{2_b}$, since the bicyclic moiety is smaller than the benzene ring, this led to a contract in the size of the ligand which reflects on its hydrophobic interactions; also, the bi-

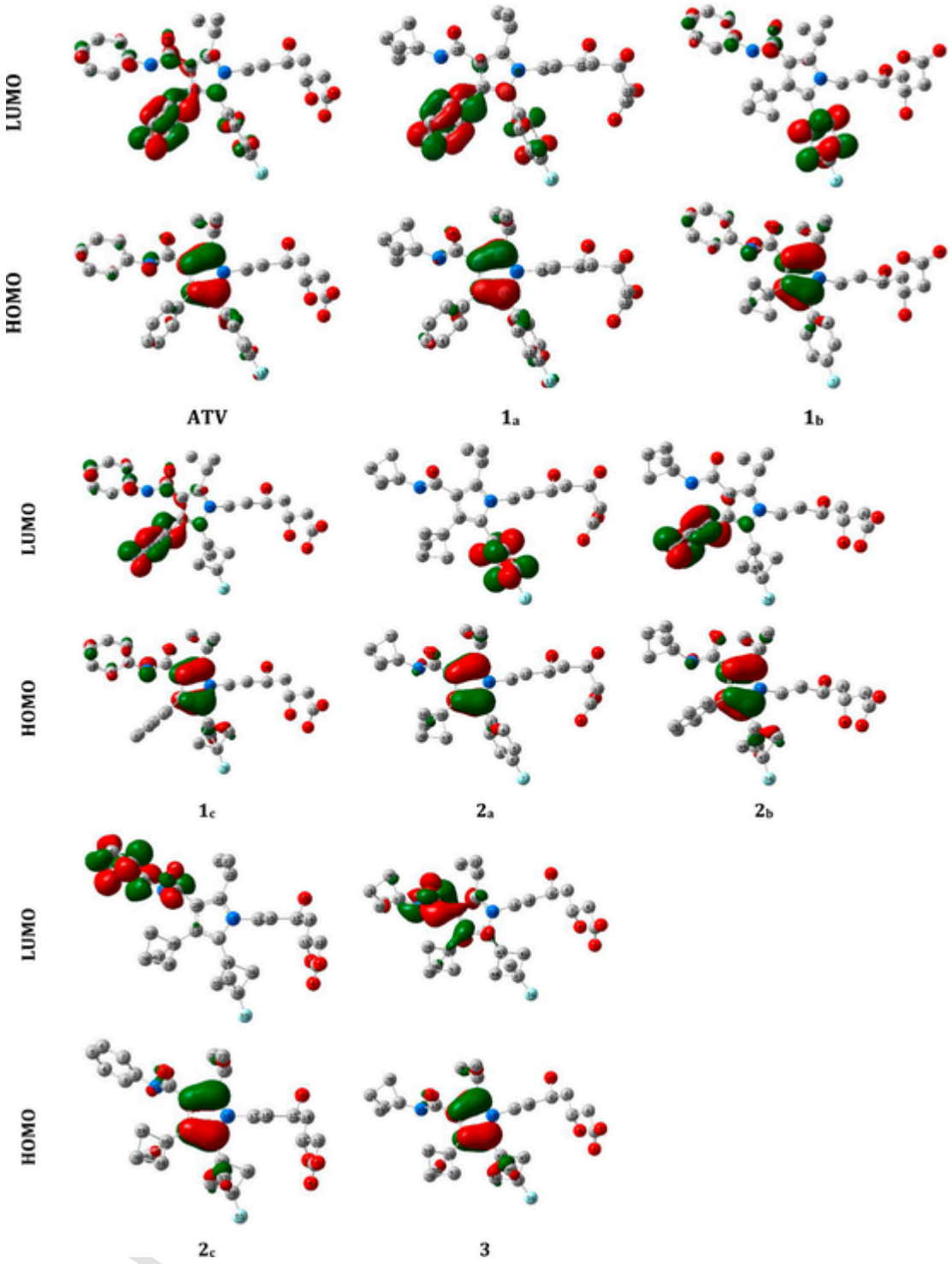

Fig. 6. Frontier molecular orbitals of atorvastatin and its analogues at CAM-B3LYP/6-31 + G*/water; Hydrogen atoms were hidden.

cyclic moiety is completely aliphatic which lead to loosing of all π – π interactions that phenyl group were able to form.

As it can be seen in Fig. 10,**1a** interactions were consistent during simulation time with the following amino acids ASP690 (almost 90% of the simulation time) LYS735 (nearly 70% of the simulation time), ASN755 (almost 60% of the simulation time), and SER565 (practically 50% of the simulation time) via H-bond and water bridge. Hydrophobic interactions with LEU853, ALA856, CYS561, ARG568, and GLY860 were observed. Fig. 11 represents the interaction with each residual during trajectories, and it shows that ASP690, GLU559, LYS735, and ASN755 are essential for ligand holding within the active site. SER565 and ARG568 interact until 65 ns and 90ns, respectively, before they lose their interactions. 2D interactions were plotted in Fig. 12.

7.2. MM-GBSA

As it can be seen from Table 7, **atorvastatin** exerts the most favored MM-GBSA energy with almost 8 kcal/mol and 17 kcal/mol dif-

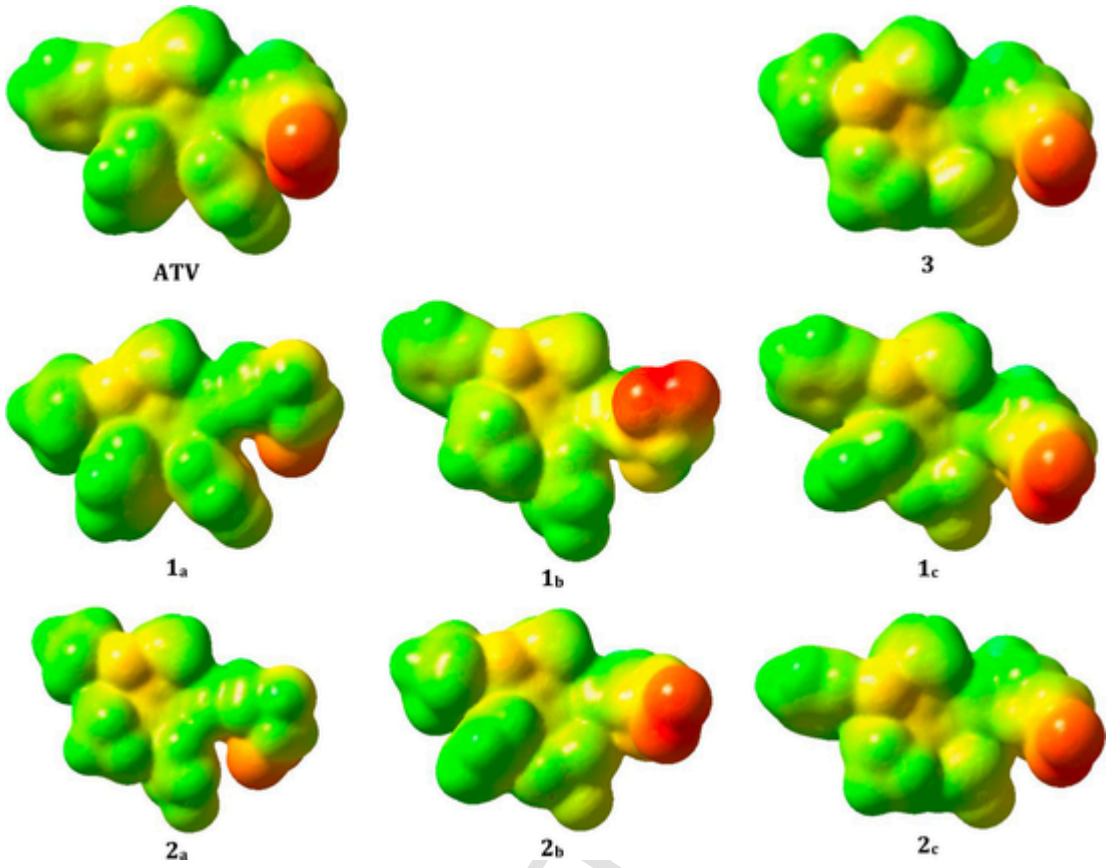

Fig. 7. The molecular electrostatic potential of atorvastatin and its analogues at CAM-B3LYP/6-31 + G*/water.

ference comparing to $\mathbf{1_a}$ and $\mathbf{2_b}$, respectively. The favored binding of **atorvastatin** is also attributed to Coulombic, Lipophilic energy, H-bonding, and vdW interactions. The packing ($\pi - \pi$ interaction) was disfavored in both analogues due to loss of the aromatic character; in contrast,$\mathbf{1_a}$ and $\mathbf{2_b}$ show more favored covalent binding energy.

8. Conclusion

In this research, we suggest seven new derivatives for **atorvastatin** via replacing the phenyl group with bicyclic[1,1,1]pentane in attempt to improve its physicochemical properties and drug-likeness. Calculations displayed that the suggest analogues molecular weight, ClogP, logS, and MR were enhanced; also, all analogues obey the rule of five with one exception MW > 500. DFT calculations showed that these compounds are thermodynamic and kinetic stable, and their reactivity and electronic properties were similar to **atorvastatin**. Analogues $\mathbf{1_a}$ and $\mathbf{2_b}$ have a docking score higher than the score exhibited by **atorvastatin**; also, docking reveals that the fluorophenyl group should not be substituted. However, molecular dynamic simulation followed by MM-GBSA calculations shows that **atorvastatin** interactions were stronger than $\mathbf{1_a}$ and $\mathbf{2_b}$ with small RMSD and higher MM-GBSA. In general, the results exhibited by $\mathbf{1_a}$were promising and can be taken further via the synthesis of this derivative and to be tested in vitro studies.

Uncited Reference

[53].

CRediT authorship contribution statement

Radwan Alnajjar: Investigation, Visualization, Writing - original draft, Writing - review & editing. **Najwa Mohamed:** Conceptualization, Methodology, Data curation. **Nagwa Kawafi:** Conceptualization, Methodology, Data curation.

Declaration of Competing Interest

None.

Supplementary materials

Supplementary material associated with this article can be found, in the online version, at doi:10.1016/j.molstruc.2020.129628.

Table 6
Docking scores of atorvastatin and its analogues with HMG-CoA reductase.

Compound	Docking score kcal /mol	Amino acid/ interaction	Distance Å	No. of hydrogen bond
ATV	-8.67	Asp690/ HB-Acceptor Ser565/ HB-Donor Lys735/ HB-Donor Arg590/HB-Donor Lys692/ H_2O Bridge Asp690/ H_2O Bridge	1.92 2.01 2.15 2.43 3.01 3.73	6
$\mathbf{1_a}$	-8.99	Glu559/ HB-acceptor Lys735/ HB-Donor Asp690/ H_2O Bridge	2.35 2.50 3.86	3
$\mathbf{1_b}$	-8.54	Lys735/ HB-Donor Ala751/ HB-Acceptor Asn755/ HB-Donor Lys691/ HB-Donor Lys692/ HB-Donor	1.91 1.92 2.27 2.36 2.44	5
$\mathbf{1_c}$	-7.60	Lys735/ HB-Donor Lys692/ H_2O Bridge Asp690/ H_2O Bridge	2.44 2.89 3.90	3
$\mathbf{2_a}$	-7.32	Asp690/HB-Acceptor Lys735/ HB-Donor Lys691/ HB-Donor	1.94 2.34 2.41	3
$\mathbf{2_b}$	-8.70	Glu559/ HB-Acceptor Arg590/ HB-Donor Lys735/ HB-donor Asn755/ HB-Donor Lys691/ HB-Donor Lys735/ HB-Donor	1.86 2.05 2.08 2.16 2.20 2.24	6
$\mathbf{2_c}$	-7.60	Lys735/ HB-Donor Lys691/ HB-Donor Asp690/ H_2O Bridge	1.80 2.31 3.84	3
3	-7.54	Lys735/ HB-Donor Lys735/ HB-Donor Asn755/ HB-Donor	1.99 2.12 2.22	3

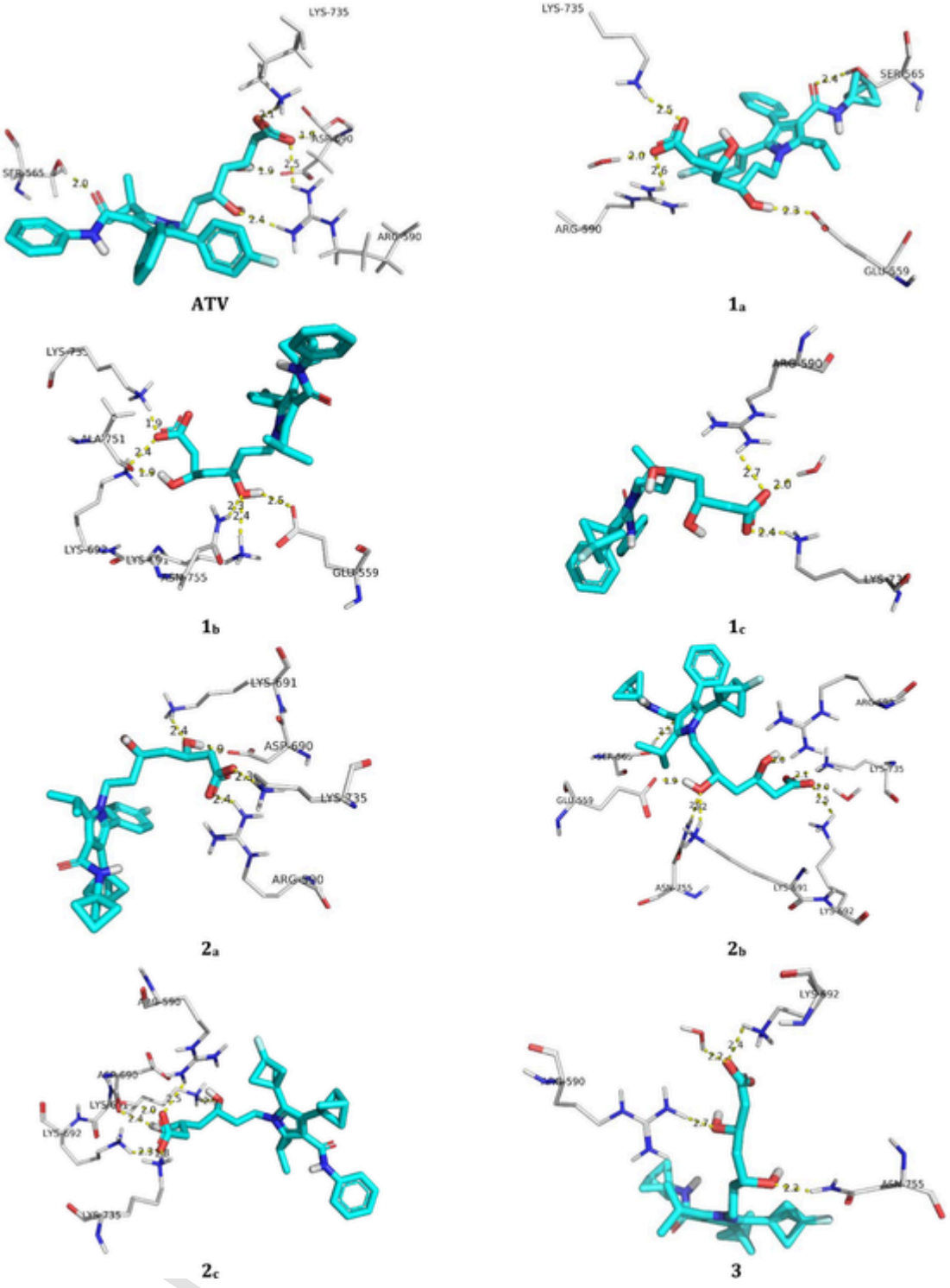

Fig. 8. Ligands interactions within the active site of HMG-COA reductase.

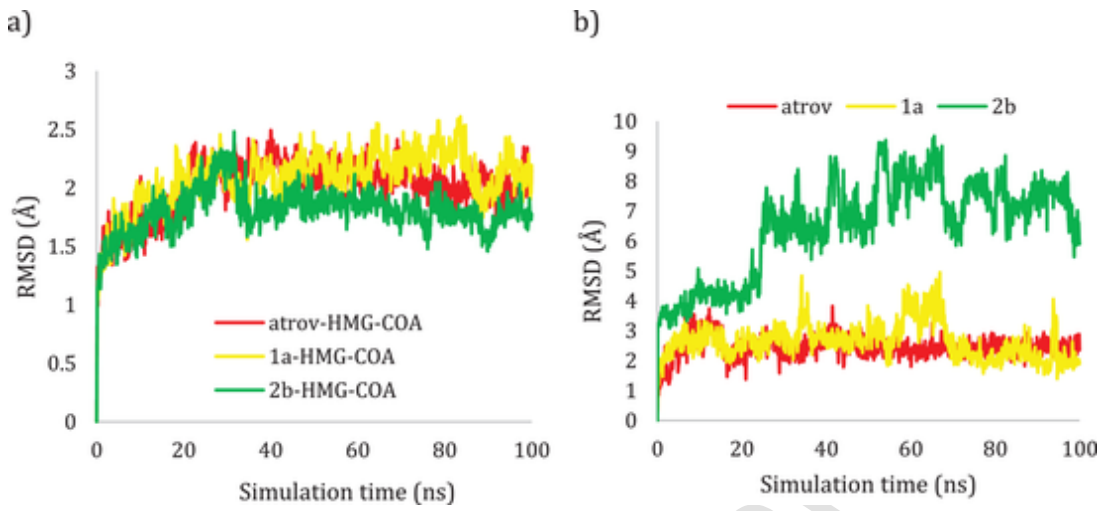

Fig. 9. A) Plots of RMSD for Cα atoms (Å) with respect to the initial structure vs simulation time (ns) for all the complexes; B) Plots of RMSD for ligand atoms (Å) with respect to the initial structure vs simulation time (ns) for all the complexes.

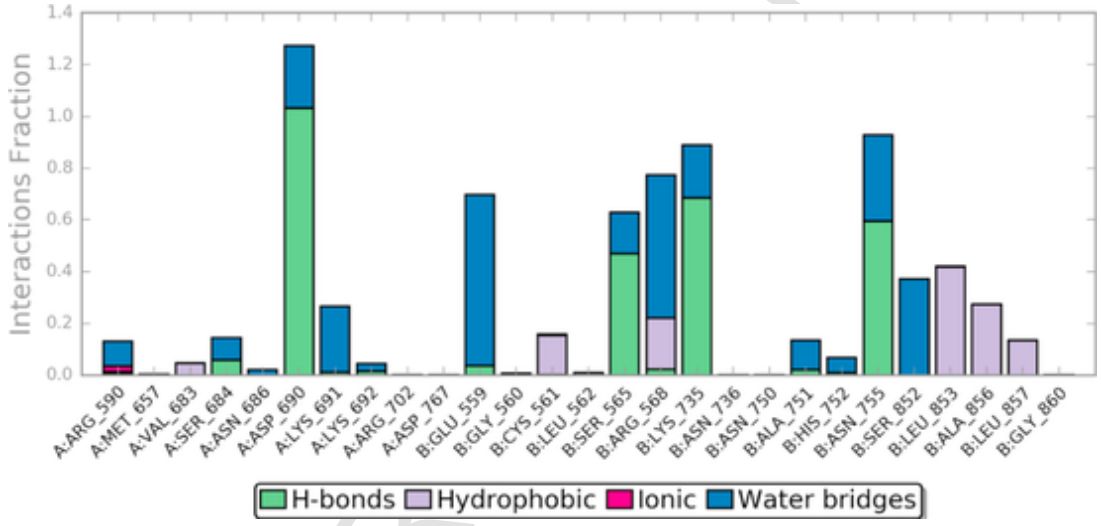

Fig. 10. The histogram of 1_a- HMG-COA contact throughout the 100ns trajectories.

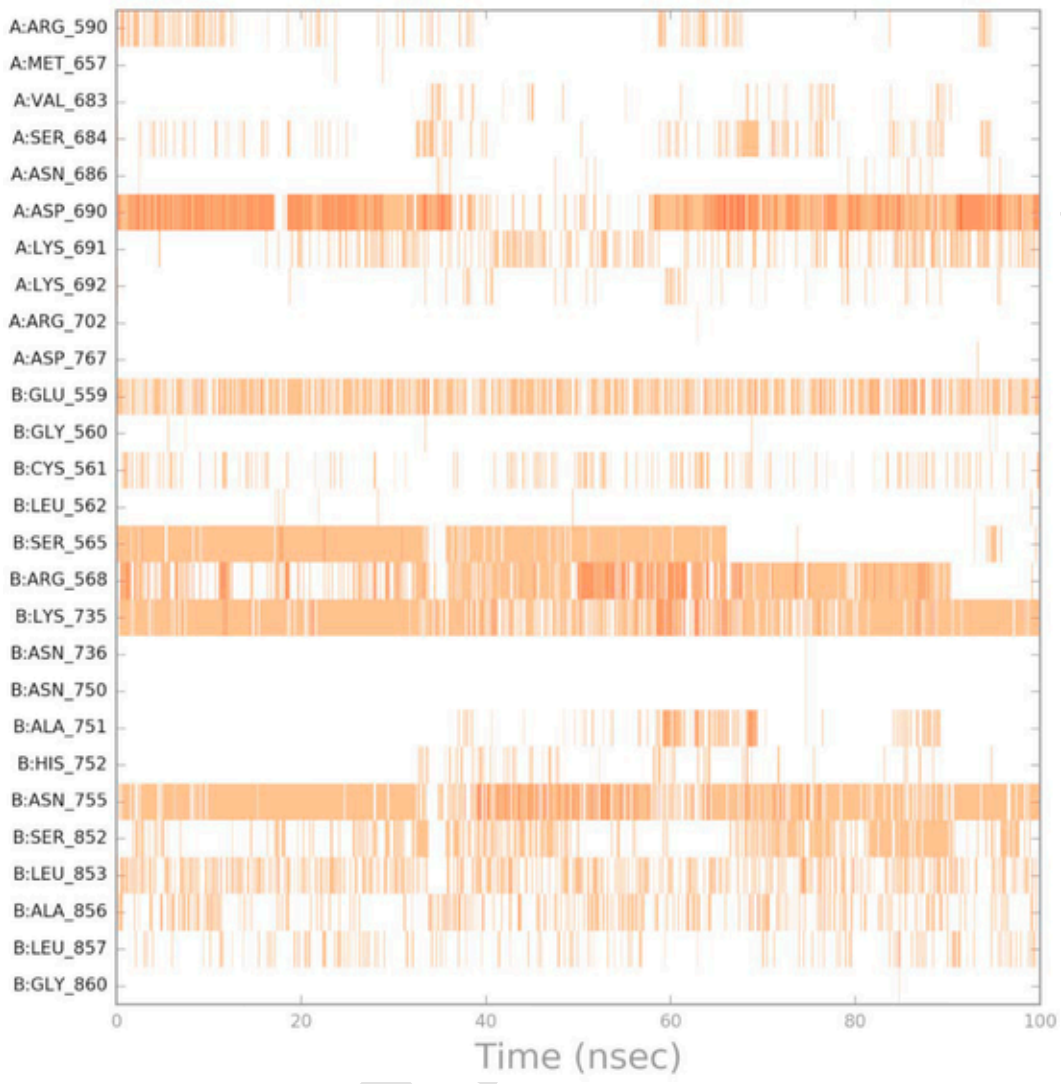

Fig. 11. 1_a- HMG-COA interaction shown by the active site amino acids in each trajectory frame, white refers to zero interaction while the deep color indicated more interactions.

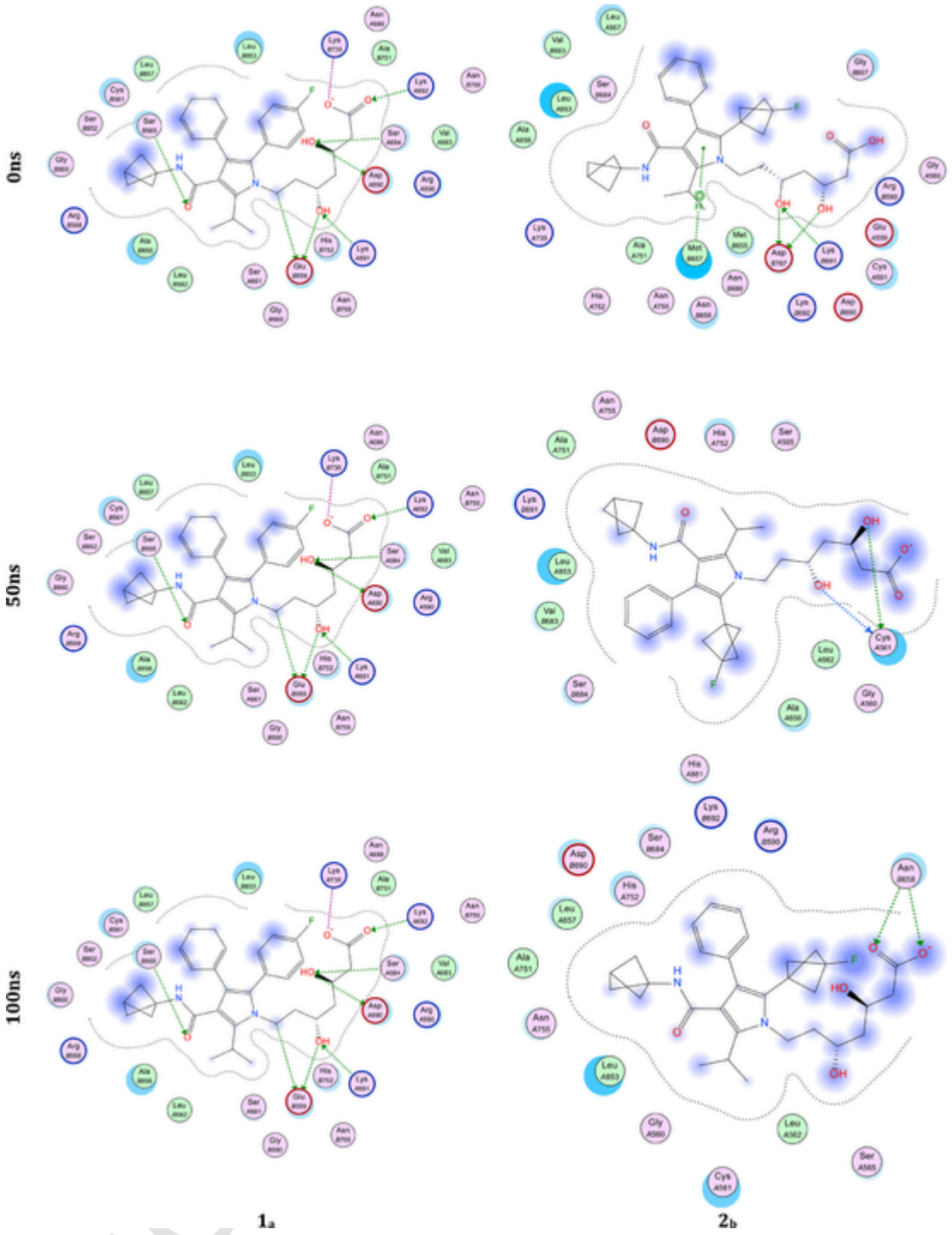

Fig. 12. 2D representation of 1_a and 2_b interaction during simulation time, snapshotted at 0, 50, and 100ns of simulation time.

Table 7
Prime MM-GBSA energies for Ligands binding at the active site of HMG-COA enzyme

	ΔG Binding	Coulomb	Covalent	H-bond	Lipo	Packing	Solv_GB	vdW
Atorvastatin	-53.49	-24.77	2.97	-3.03	-18.56	-0.85	42.22	-51.48
1_a	-45.35	-21.59	3.12	-3.01	-15.48	-0.17	39.30	-47.52
2_b	-36.36	-16.44	3.60	-1.02	-15.14	-0.57	39.73	-46.53

Coulomb: Coulomb energy; Covalent: Covalent binding energy; H-bond: Hydrogen-bonding energy; Lipo: Lipophilic energy; Packing: Pi-pi packing energy; Solv_GB: Generalized Born electrostatic solvation energy; vdW: Van der Waals energy.

References

[1] F. Taylor, M.D. Huffman, A.F. Macedo, T.H.M. Moore, M. Burke, G. Davey Smith, K. Ward, S. Ebrahim, Statins for the primary prevention of cardiovascular disease, Cochrane Database of Systematic Reviews (1) (2013).

[2] R. Vuppalanchi, N. Chalasani, Statins for hyperlipidemia in patients with chronic liver disease: are they safe?, Clinical Gastroenterology and Hepatology 4 (7) (2006) 838–839.

[3] F.J. Alenghat, A.M. Davis, Management of Blood Cholesterol, JAMA 321 (8) (2019) 800–801.

[4] M.K. Shaw, R.S. Newton, D.R. Sliskovic, B.D. Roth, E. Ferguson, B.R. Krause, Hep-G2 cells and primary rat hepatocytes differ in their response to inhibitors of HMG-CoA reductase, Biochemical and Biophysical Research Communications 170 (2) (1990) 726–734.

[5] J. Fischer, C.R. Ganellin, A. Ganesan, J. Proudfoot, Analogue-based drug discovery, Wiley-VCH Hoboken, NJ, 2010.

[6] E.S. Istvan, J. Deisenhofer, Structural Mechanism for Statin Inhibition of HMG-CoA Reductase, Science 292 (5519) (2001) 1160–1164.

[7] A. Mendieta, F. Jiménez, L. Garduño-Siciliano, A. Mojica-Villegas, B. Rosales-Acosta, L. Villa-Tanaca, G. Chamorro-Cevallos, J.L. Medina-Franco, N. Meurice, R.U. Gutiérrez, Synthesis and highly potent hypolipidemic activity of alpha-asarone-and fibrate-based 2-acyl and 2-alkyl phenols as HMG-CoA reductase inhibitors, Bioorganic & medicinal chemistry 22 (21) (2014) 5871–5882.

[8] M. Hedl, L. Tabernero, C.V. Stauffacher, V.W. Rodwell, Class II 3-hydroxy-3-methylglutaryl coenzyme A reductases, Journal of bacteriology 186 (7) (2004) 1927–1932.

[9] K. Frimpong, V.W. Rodwell, Catalysis by Syrian hamster 3-hydroxy-3-methylglutaryl-coenzyme A reductase. Proposed roles of histidine 865, glutamate 558, and aspartate 766, Journal of Biological Chemistry 269 (15) (1994) 11478–11483.

[10] D.A. Bochar, C.V. Stauffacher, V.W. Rodwell, Investigation of the conserved lysines of Syrian hamster 3-hydroxy-3-methylglutaryl coenzyme A reductase, Biochemistry 38 (48) (1999) 15848–15852.

[11] E.S. Istvan, J. Deisenhofer, The structure of the catalytic portion of human HMG-CoA reductase, Biochimica et Biophysica Acta (BBA)-Molecular and Cell Biology of Lipids 1529 (1–3) (2000) 9–18.

[12] L. Tabernero, V.W. Rodwell, C.V. Stauffacher, Crystal structure of a statin bound to a class II hydroxymethylglutaryl-CoA reductase, Journal of Biological Chemistry 278 (22) (2003) 19933–19938.

[13] K. Maggon, Best-selling human medicines 2002-2004, Drug Discovery Today 10 (11) (2005) 739–742.

[14] M.S. Rodde, G.T. Divase, T.B. Devkar, A.R. Tekade, Solubility and Bioavailability Enhancement of Poorly Aqueous Soluble Atorvastatin: In Vitro, Ex Vivo, and In Vivo Studies, BioMed Research International 2014 (2014) 463895.

[15] C.A. Briggs, R.A. Jennings, R. Wade, K. Harasawa, S. Ichikawa, K. Minohara, S. Nakagawa, Crystalline [R-(R*, R*)]-2-(4-Dfluorophenyl)-β, δ-dihydroxy-5-(1-methylethyl)-3-phenyl-4-[(phenylamino) carbonyl]-1H-pyrrole-1-heptanoic acid hemi calcium salt (atorvastatin), Google Patents: (1999).

[16] S.-G. An, Y.-T. Sohn, Crystal forms of atorvastatin, Archives of Pharmacal Research 32 (6) (2009) 933–936.

[17] W.D. Wang, X. Gao, M. Strohmeier, W. Wang, S. Bai, C. Dybowski, Solid-State NMR Studies of Form I of Atorvastatin Calcium, The Journal of Physical Chemistry B 116 (11) (2012) 3641–3649.

[18] M. Hoffmann, M. Nowosielski, DFT study on hydroxy acid-lactone interconversion of statins: the case of atorvastatin, Organic & Biomolecular Chemistry 6 (19) (2008) 3527–3531.

[19] Z. Wang, L. Cheng, Z. Kai, F. Wu, Z. Liu, M. Cai, Molecular modeling studies of atorvastatin analogues as HMGR inhibitors using 3D-QSAR, molecular docking and molecular dynamics simulations, Bioorganic & Medicinal Chemistry Letters 24 (16) (2014) 3869–3876.

[20] A.F. Stepan, C. Subramanyam, I.V. Efremov, J.K. Dutra, T.J. O'Sullivan, K.J. DiRico, W.S. McDonald, A. Won, P.H. Dorff, C.E. Nolan, S.L. Becker, L.R. Pustilnik, D.R. Riddell, G.W. Kauffman, B.L. Kormos, L. Zhang, Y. Lu, S.H. Capetta, M.E. Green, K. Karki, E. Sibley, K.P. Atchison, A.J. Hallgren, C.E. Oborski, A.E. Robshaw, B. Sneed, C.J. O'Donnell, Application of the Bicyclo[1.1.1]pentane Motif as a Nonclassical Phenyl Ring Bioisostere in the Design of a Potent and Orally Active γ-Secretase Inhibitor, Journal of Medicinal Chemistry 55 (7) (2012) 3414–3424.

[21] P.K. Mykhailiuk, Saturated bioisosteres of benzene: where to go next?, Organic & Biomolecular Chemistry 17 (11) (2019) 2839–2849.

[22] R. Pellicciari, M. Raimondo, M. Marinozzi, B. Natalini, G. Costantino, C. Thomsen, (S-+)-2-(3'-Carboxybicyclo[1.1.1]pentyl)- glycine, a Structurally New Group I Metabotropic Glutamate Receptor Antagonist, Journal of Medicinal Chemistry 39 (15) (1996) 2874–2876.

[23] C.A. Lipinski, Lead- and drug-like compounds: the rule-of-five revolution. Drug discovery today, Technologies 1 (4) (2004) 337–341.

[24] A.K. Ghose, V.N. Viswanadhan, J.J. Wendoloski, A knowledge-based approach in designing combinatorial or medicinal chemistry libraries for drug discovery. 1. A qualitative and quantitative characterization of known drug databases, Journal of combinatorial chemistry 1 (1) (1999) 55–68.

[25] D.F. Veber, S.R. Johnson, H.-Y. Cheng, B.R. Smith, K.W. Ward, K.D. Kopple, Molecular properties that influence the oral bioavailability of drug candidates, Journal of medicinal chemistry 45 (12) (2002) 2615–2623.

[26] R. Brenk, A. Schipani, D. James, A. Krasowski, I.H. Gilbert, J. Frearson, P.G. Wyatt, Lessons learnt from assembling screening libraries for drug discovery for neglected diseases, ChemMedChem 3 (3) (2008) 435.

[27] C.A. Lipinski, F. Lombardo, B.W. Dominy, P.J. Feeney, Experimental and computational approaches to estimate solubility and permeability in drug discovery and development settings, Advanced drug delivery reviews 23 (1–3) (1997) 3–25.

[28] I.V. Tetko, P. Bruneau, H.-W. Mewes, D.C. Rohrer, G.I. Poda, Can we estimate the accuracy of ADME–Tox predictions?, Drug discovery today 11 (15–16) (2006) 700–707.

[29] F. Montanari, G.F. Ecker, Prediction of drug–ABC-transporter interaction—Recent advances and future challenges, Advanced drug delivery reviews 86 (2015) 17–26.

[30] B. Testa, S.D. Kraemer, The Biochemistry of Drug Metabolism–An Introduction-Testa-2007-Chemistry & Biodiversity-Wiley Online Library, Chem. Biodivers 4 (3) (2007).

[31] J. Kirchmair, A.H. Göller, D. Lang, J. Kunze, B. Testa, I.D. Wilson, R.C. Glen, G. Schneider, Predicting drug metabolism: experiment and/or computation?, Nature reviews Drug discovery 14 (6) (2015) 387–404.

[32] Inc., C. C. G., Molecular operating environment (MOE), Chemical Computing Group Inc 1010 Sherbooke St. West, Suite# 910, Montreal, 2016.

[33] S. Release, 3: Desmond molecular dynamics system, DE Shaw research, New York, NY, 2017. Maestro-Desmond Interoperability Tools, Schrödinger, New York, NY, 2017.

[34] E. Harder, W. Damm, J. Maple, C. Wu, M. Reboul, J.Y. Xiang, L. Wang, D. Lupyan, M.K. Dahlgren, J.L. Knight, J.W. Kaus, D.S. Cerutti, G. Krilov, W.L. Jorgensen, R. Abel, R.A. Friesner, OPLS3: A Force Field Providing Broad Coverage of Drug-like Small Molecules and Proteins, Journal of Chemical Theory and Computation 12 (1) (2016) 281–296.

[35] W.L. Jorgensen, J. Chandrasekhar, J.D. Madura, R.W. Impey, M.L. Klein, Comparison of simple potential functions for simulating liquid water, The Journal of Chemical Physics 79 (2) (1983) 926–935.

[36] E. Neria, S. Fischer, M. Karplus, Simulation of activation free energies in molecular systems, The Journal of Chemical Physics 105 (5) (1996) 1902–1921.

[37] S.d. Release, 4. Desmond Molecular Dynamics System, DE Shaw Research, Maestro-Desmond Interoperability Tools, 2016.

[38] G.J. Martyna, M.L. Klein, M. Tuckerman, Nosé–Hoover chains: The canonical ensemble via continuous dynamics, The Journal of Chemical Physics 97 (4) (1992) 2635–2643.

[39] G.J. Martyna, D.J. Tobias, M.L. Klein, Constant pressure molecular dynamics algorithms, The Journal of Chemical Physics 101 (5) (1994) 4177–4189.

[40] M.J. Waring, Defining optimum lipophilicity and molecular weight ranges for drug candidates—molecular weight dependent lower log D limits based on permeability, Bioorganic & medicinal chemistry letters 19 (10) (2009) 2844–2851.

[41] G.L. Patrick, An introduction to medicinal chemistry, Oxford university press, 2013.

[42] P. Ertl, B. Rohde, P. Selzer, Fast calculation of molecular polar surface area as a sum of fragment-based contributions and its application to the prediction of drug transport properties, Journal of medicinal chemistry 43 (20) (2000) 3714–3717.

[43] J.A. Arnott, S.L. Planey, The influence of lipophilicity in drug discovery and design, Expert opinion on drug discovery 7 (10) (2012) 863–875.

[44] R. Mannhold, G.I. Poda, C. Ostermann, I.V. Tetko, Calculation of molecular lipophilicity: State-of-the-art and comparison of log P methods on more than 96,000 compounds, Journal of pharmaceutical sciences 98 (3) (2009) 861–893.

[45] J.D. Hughes, J. Blagg, D.A. Price, S. Bailey, G.A. DeCrescenzo, R.V. Devraj, E. Ellsworth, Y.M. Fobian, M.E. Gibbs, R.W. Gilles, Physiochemical drug properties associated with in vivo toxicological outcomes, Bioorganic & medicinal chemistry letters 18 (17) (2008) 4872–4875.

[46] T.J. Ritchie, S.J.F. Macdonald, S. Peace, S.D. Pickett, C.N. Luscombe, Increasing small molecule drug developability in sub-optimal chemical space, MedChemComm 4 (4) (2013) 673–680.

[47] G. Ottaviani, D.J. Gosling, C. Patissier, S. Rodde, L. Zhou, B. Faller, What is modulating solubility in simulated intestinal fluids?, European journal of pharmaceutical sciences 41 (3–4) (2010) 452–457.

[48] K.T. Savjani, A.K. Gajjar, J.K. Savjani, Drug solubility: importance and enhancement techniques, ISRN pharmaceutics (2012) 2012.

[49] H. Veith, N. Southall, R. Huang, T. James, D. Fayne, N. Artemenko, M. Shen, J. Inglese, C.P. Austin, D.G. Lloyd, Comprehensive characterization of cytochrome P450 isozyme selectivity across chemical libraries, Nature biotechnology 27 (11) (2009) 1050.

[50] R.O. Potts, R.H. Guy, Predicting skin permeability, Pharmaceutical research 9 (5) (1992) 663–669.

[51] C.-G. Zhan, J.A. Nichols, D.A. Dixon, Ionization Potential, Electron Affinity, Electronegativity, Hardness, and Electron Excitation Energy: Molecular Properties from Density Functional Theory Orbital Energies, The Journal of Physical Chemistry A 107 (20) (2003) 4184–4195.

[52] L.R. Domingo, M.J. Aurell, P. Pérez, R. Contreras, Quantitative characterization of the global electrophilicity power of common diene/dienophile pairs in Diels–Alder reactions, Tetrahedron 58 (22) (2002) 4417–4423.

[53] M. Fesatidou, A. Petrou, G. Athina, Heterocycle compounds with antimicrobial activity, Current Pharmaceutical Design 26 (8) (2020) 867–904.